HAL
open science

Edge states in a boundary layer

Stefania Cherubini, Pietro de Palma, Jean-Christophe Robinet, Alessandro Bottaro

To cite this version:

Stefania Cherubini, Pietro de Palma, Jean-Christophe Robinet, Alessandro Bottaro. Edge states in a boundary layer. Physics of Fluids, 2011, 23 (051705), pp.4. 10.1063/1.3589842 . hal-00799788

HAL Id: hal-00799788

https://hal.science/hal-00799788

Submitted on 13 Mar 2013

HAL is a multi-disciplinary open access archive for the deposit and dissemination of scientific research documents, whether they are published or not. The documents may come from teaching and research institutions in France or abroad, or from public or private research centers.

L'archive ouverte pluridisciplinaire **HAL**, est destinée au dépôt et à la diffusion de documents scientifiques de niveau recherche, publiés ou non, émanant des établissements d'enseignement et de recherche français ou étrangers, des laboratoires publics ou privés.

Edge states in a boundary layer

S. Cherubini,[1] P. De Palma,[1] J.-Ch. Robinet,[2] and A. Bottaro[3]
[1]*DIMeG, CEMeC, Politecnico di Bari, Via Re David 200, Bari 70125, Italy*
[2]*DynFluid Laboratory, Arts et Metiers ParisTech, 151 Bd. de l'Hôpital, Paris 75013, France*
[3]*DICAT, Università di Genova, via Montallegro 1, Genova 16145, Italy*

(Received 10 February 2011; accepted 20 April 2011; published online 23 May 2011)

The understanding of laminar-turbulent transition in shear flows has recently progressed along new paradigms based on the central role of nonlinear exact coherent states. We follow such paradigms to identify, for the first time in a spatially developing flow, localized flow structures living on the edge of chaos, which are the precursors of turbulence. These coherent structures are constituted by hairpin vortices and streamwise streaks. The results reported here extend the dynamical systems description of transition to spatially developing flows. © *2011 American Institute of Physics*. [doi:10.1063/1.3589842]

Recent progress in understanding transition to turbulence has been boosted by a new vision rooted onto dynamical systems theory in which transition and turbulence stem from the apparently random bounce of the system's trajectory among mutually repelling flow states, which are exact, albeit unstable, solutions of the Navier-Stokes (NS) equations.[1–6] Some of these solutions, called *edge states*, live in phase-space on the boundary between the laminar and the turbulent states (the edge of turbulence), acting as relative attractors for the states evolving along their stable manifold.[7–9] Evidence for the validity of such a description of transition has been found for the cases of parallel flows such as pipe, plane Couette and Poiseuille flows, with periodic conditions in the streamwise direction.[2,4,6,9,10] Very recently, localized solutions have been found[9,11–14] which appear to be relevant to describe the onset of transition induced by disturbances which grow and, eventually, invade the flow in the form of turbulent spots. In the present letter, we extend the concept of edge of turbulence to a spatially developing flow, such as the boundary-layer flow over a flat plate, aiming to identify some of the structures living on it. The results of the present analysis suggest the existence of relative attractors which are formed by hairpin vortices and streamwise streaks.

The stability of a boundary-layer flow over a flat plate has been analyzed numerically, the Reynolds number being defined as $Re = U_\infty \delta^*/\nu$, where ν, δ^*, and U_∞ are the kinematic viscosity, the inflow boundary-layer displacement thickness, and the freestream velocity of the Blasius base flow, respectively. The nondimensional NS equations are integrated by a second-order-accurate fractional step method.[16] A domain with $L_x = 2000$, $L_y = 20$, and $L_z = 10.5$ has been chosen, x, y, and z being the streamwise, the wall-normal, and the spanwise directions, respectively. The inlet of the computational domain is located at $x_{in} = 200$. Boundary conditions are set as follows: the Blasius velocity profiles has been imposed at the inlet; a convective condition at the outlet; the no-slip condition at the bottom wall; the Blasius wall normal velocity and zero vorticity at the upper boundary points; finally, periodicity is imposed in the spanwise direction. After a grid-convergence analysis, a mesh made up by $7001 \times 150 \times 61$ points – stretched in the wall-normal direction – has been selected. The trajectories on the edge have been computed at $Re = 610$ following the shooting procedure proposed by Skufca *et al.*[7] For spatially developing boundary-layer flows, the Reynolds number increases along the streamwise direction and it may happen that the flow becomes supercritical with respect to Tollmien-Schlichting (TS) waves. This is indeed our case, since the flow is already supercritical for $Re = 610$. As a consequence, the definition of the edge of turbulence needs to be generalized with respect to that employed for the analysis of stable parallel base flows,[17] and thus we define the edge of turbulence as the dividing set in phase space between trajectories which go to turbulence at "short times" with the perturbation energy increasing monotonically, and those which experience a substantial drop of the perturbation amplitude and energy, and eventually go to turbulence following a "long time" path because of the amplification of TS waves. Phase-space trajectories closely approximating the edge are computed initializing the flow using the linear and non-linear optimal perturbations provided in Ref. 18 (see Figs. 3 and 4 therein), the perturbation vector $\mathbf{u} = (u, v, w)^T$ being defined with respect to the spatially developing Blasius flow. These optimal perturbations, computed in order to allow an optimal growth of the energy at short times, show different features and symmetries. In particular, the linear optimal is characterized by vortices aligned with the streamwise direction, whereas the non-linear optimal contains spanwise-inclined vortices. This distinction is believed to be crucial for the subsequent evolution of the flow. Following the procedure provided in Refs. 7 and 19, a bisection method is employed. The value of the initial energy $E_0 = \langle \mathbf{u}(t=0) \cdot \mathbf{u}(t=0) \rangle$ (where the symbol $\langle\rangle$ indicates integration over the computational domain) is determined such that the trajectory of the flow evolves freely along the boundary between the laminar and the turbulent state, unraveling the structure of the edge attractor. Since we are dealing with localized perturbations which spread in space, the time history of their global energy does not characterize well their local amplitude evolution. For this reason,

 © 2011 American Institute of Physics

Author complimentary copy. Redistribution subject to AIP license or copyright, see http://phf.aip.org/phf/copyright.jsp

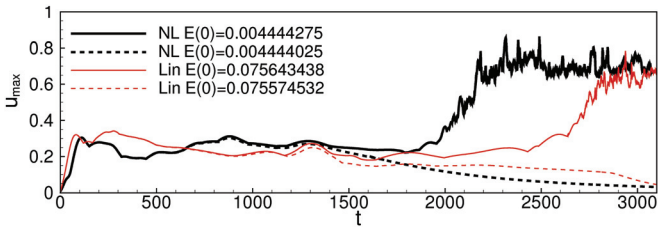

FIG. 1. (Color online) Streamwise disturbance velocity peaks versus time for DNSs initialized by the linear (thin gray lines, red online) and the nonlinear optimal perturbation (black thick lines) for different values of the initial energy.

we use the peak value of the streamwise component of the perturbation, u_{max}, to track the disturbance on the edge. This variable is plotted in Fig. 1 for four different trajectories following the edge for about 1200 time units, from $t \approx 100$ to $t \approx 1300$. In the non-linear case, the edge is found for a lower initial energy ($E_0 \approx 0.00444$) than that needed by the linear optimal perturbation ($E_0 \approx 0.0756$). The values of u_{max} achieved on the edge trajectories are of the same order for the two initializations, indicating that the lower disturbance energy level attained by the nonlinear optimal is related to its spatial compactness at small times. The irregular time history of u_{max} suggests the presence of a complex chaotic attractor living on the edge. Such a non-smooth behaviour is very similar to that found in pipe[11] and plane Couette[12] flows in large domains. It is noteworthy that, for such cases, localized flow structures have been found to characterize the edge state.

Therefore, the perturbation on the nonlinear edge trajectory (solid black thick line in Fig. 1) has been analyzed in order to ascertain the existence of an attracting structure. Fig. 2 shows the surfaces of the streamwise component of the velocity perturbation and of the Q-criterion, identifying the vortical structures within the flow at $t = 300$ and $t = 700$, two values of time sufficiently large to render the influence of the initial perturbation negligible. The disturbance is characterized by a main hairpin vortex placed at the leading edge of the packet, followed by a population of quasi-streamwise vortices (green surfaces), some of them presenting an inclination on their dowstream part, inducing secondary hairpin structures and streaks close to the wall (blue surfaces). The localized wave packet increases its size

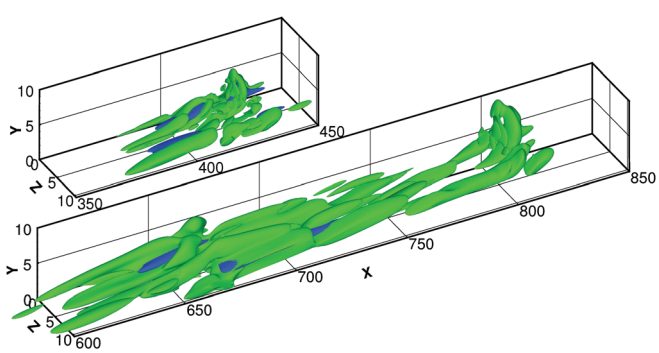

FIG. 2. (Color online) Snapshots of the streamwise component of the perturbation (darker surfaces, blue online, for $u = -0.13$) and of the Q-criterion (lighter surfaces, green online) at $t = 300$ and $t = 700$ (top and bottom, respectively) obtained by the DNS initialized with the nonlinear optimal perturbation with $E_0 = 0.004444275$.

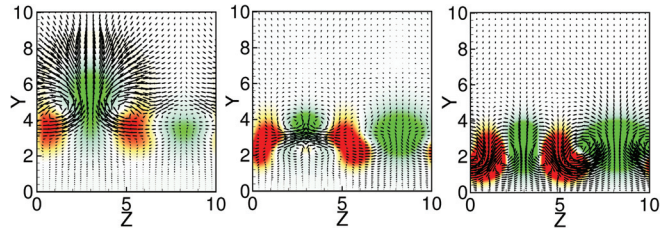

FIG. 3. (Color online) Contours of the streamwise components of the perturbation and cross-stream velocity vectors at $x = 650$ and $t = 540, 590, 660$ (from left to right) obtained using the DNS initialized by the nonlinear optimal perturbation with $E_0 = 0.004444275$ (maximum value, $v = 0.018$). Shaded contours represent values from $u = -0.06$ (lighter contours, green online) to $u = 0.04$ (darker contours, red online) (enhanced online). [URL: http://dx.doi.org/10.1063/1.3589842.1]

in the streamwise direction while it is convected downstream by the mean flow. The spatial spreading of the edge structure is due to the spatial development of the Blasius flow, which induces an increase with time of the local Reynolds number at the "center" of the wave packet. This is a crucial difference with respect to the case of localized edge structures in plane Couette or pipe flows[12,14] and explains why in this case the edge of turbulence cannot be studied by monitoring only the energy of the disturbance, but another measure is needed. Normalizing the abscissa with respect to the center of mass of the packet, computed on the basis of the energy as $X_m = \sum_i \mathcal{E}_i x_i / \sum_i \mathcal{E}_i$, where i indicates the grid points in the streamwise direction and $\mathcal{E}_i = u_i^2 + v_i^2 + w_i^2$ is the local perturbation energy, we recover a wave packet which maintains a quasi self-similar shape as it evolves in time. The presence of this weakly varying flow structure, living on the edge of turbulence, suggests the existence of a relative chaotic attractor embedded in the edge, like in the case of pipe flows[11,19] and Couette flows in very long domains.[12,14] The hairpin flow structure strongly resembles the exact coherent solution in plane Couette flow recently found in Ref. 10, indicating that coherent structures of this type could be embedded within the edge state of boundary-layer flows. Similar hairpin structures have been also experimentally recovered on the edge of turbulence in pipe flows.[20]

The hairpin vortices are also visualized in Fig. 3 which provides snapshots of the perturbation taken at the abscissa $x = 650$ for three time instants (the corresponding video shows the whole time sequence from $t = 500$ to 700). The first frame of Fig. 3 shows the typical signature of the head of the main hairpin vortex; the following one shows a pair of Λ-vortices at their joining point; the third one shows the signatures of two pairs of quasi-streamwise vortices turning into small hairpin structures. It is interesting that these structures present a symmetry with respect to the wall-normal direction, indicating that the streaks are undergoing oscillations of varicose type. Moreover, low- and high-momentum zones at the leading edge of the wave packet (first frame) are placed quite away from the wall and move closer to the wall at the trailing edge (third frame). This is related to the finite inclination of the wave packet with respect to the streamwise direction, a feature typical of turbulent spots in boundary layers. In particular, by visualizing the streamwise component of the perturbation on a side view (the first frame of

Author complimentary copy. Redistribution subject to AIP license or copyright, see http://phf.aip.org/phf/copyright.jsp

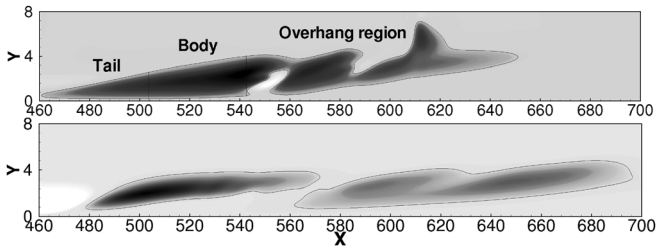

FIG. 4. Contours of the streamwise components of the perturbation (solid lines for $u = -0.02$) at $z = 2$ and $t = 500$ obtained using the DNS initialized by the nonlinear optimal perturbation with $E_0 = 0.004444275$ (top) and by the linear optimal one for $E_0 = 0.075643438$ (bottom).

Fig. 4 shows the section at $z = 2$), one can notice that the wave packet is composed by an *overhang region* at the leading edge, a body and a long tail at the upstream end of the disturbance. This pattern recalls very closely the structure of turbulent spots visualized in experiments[21] and simulations.[22] Moreover, the leading edge of the wave packet is convected downstream at a larger velocity than the trailing edge, i.e., $U_{lead} = 0.87U_\infty$ and $U_{trail} = 0.53U_\infty$, the presence of the main hairpin vortex at the leading edge explaining the large value of U_{lead}. Remarkably, such values of velocity are very close to the advection velocities of the edges of a turbulent spot.[22] All of these features induce to identify the wave packet living on the edge of turbulence as the precursor of a turbulent spot.

Different structures can be identified on the edge when the flow is initialized by the linear optimal disturbance. The perturbation on the edge trajectory has been extracted from the DNS corresponding to the solid thin gray line (red online) in Fig. 1. Fig. 5 shows the surfaces of the streamwise component of the velocity perturbation and of the Q-criterion, identifying the vortical structures within the flow at $t = 300$ and $t = 700$. The disturbance is characterized by quasi-streamwise vortices (green surfaces), on the flanks of two low-velocity streaks (blue surfaces) modulated in x. These structures are clearly visualized in Figure 6 which shows snapshots of the perturbation taken at the abscissa $x = 650$ for three time instants (the corresponding video shows the whole time sequence from $t = 500$ to 700). All of the three sections show two low- and two high-velocity streaks, induced by pairs of quasi-streamwise vortices, with strong oscillations in the spanwise direction. The high-momentum zones are placed

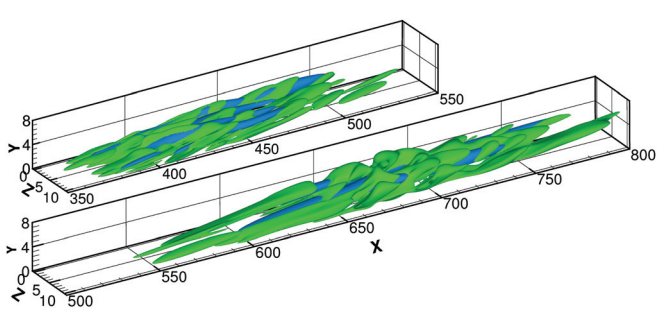

FIG. 5. (Color online) Snapshots of the streamwise component of the perturbation (darker surfaces, blue online, for $u = -0.07$) and of the Q-criterion (lighter surfaces, green online) at $t = 300$, 700 (top and bottom, respectively) obtained using the DNS initialized by the linear optimal perturbation by $E_0 = 0.075643438$.

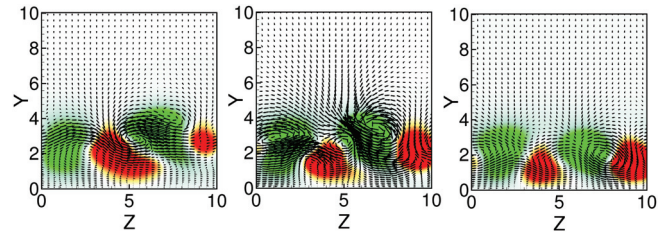

FIG. 6. (Color online) Contours of the streamwise components of the perturbation and cross-stream velocity vectors at $x = 650$ and $t = 610$, 640, 660 (from left to right) obtained using a DNS initialized by the linear optimal perturbation with $E_0 = 0.075643438$ (maximum value, $w = 0.015$). Shaded contours represent values from $u = -0.06$ (lighter contours, green online) to $u = 0.04$ (darker contours, red online) (enhanced online). [URL: http://dx.doi.org/10.1063/1.3589842.2]

closer to the wall than the low-momentum ones; however, the streaks are placed at a lower wall distance than in the nonlinear case. Moreover, the wave packet does not show a noticeable angle with respect to the streamwise direction, meaning that a "overhang region" is not present, as also shown in the second frame of Fig. 4. It is also interesting that, unlike the wave packet previously analyzed, these structures do not present any symmetry with respect to the wall-normal direction, indicating that the streaks undergo sinuous-type oscillations. The advection velocities recovered for such an edge structure are $U_{lead} = 0.72U_\infty$ and $U_{trail} = 0.55U_\infty$; thus, this wave packet has a lower spreading rate than the previous one, and this is probably due to the absence of hairpin vortices. The presence of two different flow structures living on the edge of turbulence suggests the existence of at least two different embedded relative attractors.

Finally, in order to study the evolution of disturbances in the proximity of the laminar-turbulent boundary, we visualize the chaotic attractors in phase space by tracking the trajectory of the perturbations. For the case of parallel flows such as the plane Couette flow,[23] the dissipation rate and the energy input are usually chosen as state variables, both based on L_2 norms. In the present case, due to the non-parallelism of the flow, an L_∞ norm appears appropriate. Therefore, following the theoretical work in Ref. 24, the maximum values of the three components of the velocity have been chosen as state variables. The left frame of Fig. 7 shows a trajectory following the laminar-turbulent boundary (black thick curve) as well as the trajectory of the nonlinear optimal perturbation with $E_0 = 0.1$ (thin gray line, red online) rapidly leading the flow to turbulence. The two trajectories highlight the more complex structure of the turbulent attractor (top right of the frame) with respect to the relative attractor corresponding to the edge state associated with lower amplitude levels. The latter repels any perturbation living outside the edge surface, influencing their route toward turbulence. Indeed, depending on its initial energy and shape, the perturbation may spend a considerable amount of time wandering around the attractor or its route to turbulence may be strongly deviated when passing in the neighbourhood of the edge state.[11,15] A similar dynamics is recovered for an initial linear optimal disturbance, as shown in the right frame of Fig. 7, but the trajectories on the edge (see insets of the two frames) appear quite different.

Author complimentary copy. Redistribution subject to AIP license or copyright, see http://phf.aip.org/phf/copyright.jsp

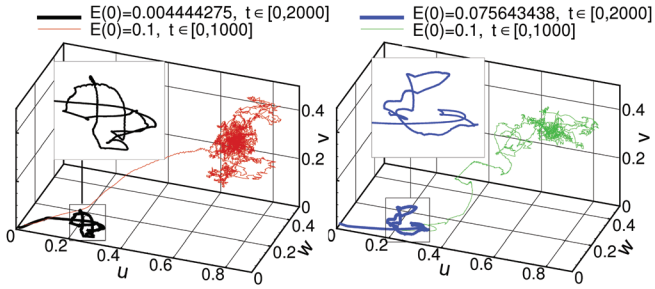

FIG. 7. (Color online) Trajectories in the phase space spanned by the maximum values of the three components of the perturbation, for simulations initialized by the nonlinear (left frame) and linear (right frame) optimal perturbations, respectively. Insets show close-ups of trajectories on the edge.

These results lead to the conclusion that, in the case of the spatially developing boundary layer, relative attractors exist which are embedded in the edge of turbulence. Remarkable differences have been found between the edge structures identified for two different initial disturbances, indicating that the edge state for the boundary layer is not unique. The edge structure reached by a linear optimal perturbation requires a (relatively) large initial energy level to be reached, and it is less efficient in spreading out in space/time. We call this the "streak-dominated edge state." On the other hand, the one induced by the nonlinear optimal perturbation follows a low-energy route to transition and is very efficient in inducing and spreading out turbulence. This is defined the "hairpin-dominated edge state." The shape of the wave packet and its advection velocities indicate that the edge state reached by the nonlinear optimal perturbation is the precursor of a turbulent spot. The spatial spreading of such a coherent structure leads to the formation of a *spot* and signals the initiation of turbulence; this occurs when the system's trajectory abandons the edge surface and follows the low-dimensional unstable manifold which leads to turbulence. The presence of the slowly varying, unstable flow structures found here suggests the existence of localized exact coherent states embedded in the edge for the case of spatially developing boundary layers.

[1]M. Nagata, "Three-dimensional traveling-wave solutions in plane Couette flow," Phys. Rev. E **55**, 2023 (1997).
[2]F. Waleffe, "Three-dimensional states in plane shear flow," Phys. Rev. Lett. **81**, 4140 (1998).
[3] H. Faisst and B. Eckhardt, "Travelling waves in pipe flow," Phys. Rev. Lett. **91**, 224502 (2003).
[4]F. Waleffe, "Homotopy of exact coherent structures in plane shear flows," Phys. Fluids **15**, 1517 (2003).
[5]B. Hof, C. van Doorne, J. Westerweel, F. Nieuwstadt, H. Faisst, B. Eckhardt, H. Wedin, R. Kerswell, and F. Waleffe, "Experimental observation of nonlinear traveling waves in turbulent pipe flow," Science **305**, 1594 (2004).
[6]B. Eckhardt, T. M. Schneider, B. Hof, and J. Westerweel, "Turbulence transition of pipe flow," Annu. Rev. Fluid Mech. **39**, 447 (2007).
[7]J. D. Skufca, J. Yorke, and B. Eckhardt, "Edge of chaos in a parallel shear flow," Phys. Rev. Lett. **96**, 174101 (2006).
[8]T. M. Schneider, J. F. Gibson, M. Lagha, F. De Lillo, and B. Eckhardt, "Laminar-turbulent boundary in plane Couette flow," Phys. Rev. E **78**, 037301 (2008).
[9]T. M. Schneider, J. F. Gibson, and J. Burke, "Snakes and ladders: Localized solutions of plane Couette flow," Phys. Rev. Lett. **104**, 104501 (2010).
[10]T. Itano and S. C. Generalis, "Hairpin vortex solution in planar Couette flow: A tapestry of knotted vortices," Phys. Rev. Lett. **102**, 114501 (2009).
[11]F. Mellibovsky, A. Meseguer, T. M. Schneider, and B. Eckhardt, "Transition in localized pipe-flow turbulence," Phys. Rev. Lett. **103**, 054502 (2009).
[12]Y. Duguet, P. Schlatter, and D. S. Henningson, "Localized edge states in plane Couette flow," Phys. Fluids **21**, 111701 (2009).
[13]A. P. Willis and R. R. Kerswell, "Turbulent dynamics and pipe flow captured in a reduced model: Puff relaminarization and localized edge states," J. Fluid Mech. **619**, 213 (2009).
[14]T. M. Schneider, D. Marinc, and B. Eckhardt, "Localised edge states nucleate turbulence in extended plane Couette cells," J. Fluid Mech. **646**, 441 (2010).
[15]Y. Duguet, L. Brandt, and B. R. J. Larsson, "Towards minimal perturbations in transitional plane Couette flow," Phys. Rev. E **82**, 026316 (2010).
[16]R. Verzicco and P. Orlandi, "A finite-difference scheme for the three-dimensional incompressible flows in cylindrical coordinates," J. Comput. Phys. **123**, 402 (1996).
[17]Y. Duguet, A. P. Willis, and R. R. Kerswell, "Transition in pipe flow: The saddle structure on the boundary of turbulence," J. Fluid Mech. **613**, 255 (2008).
[18]S. Cherubini, P. De Palma, J. Robinet, and A. Bottaro, "Rapid path to transition via non-linear localized optimal perturbations in a boundary-layer flow," Phys. Rev. E **82**, 066302 (2010).
[19]T. M. Schneider, B. Eckhardt, and J. Yorke, "Turbulence transition and the edge of chaos in pipe flow," Phys. Rev. Lett. **99**, 034502 (2007).
[20]Y. Tasaka, T. M. Schneider, and T. Mullin, "Folded edge of turbulence in a pipe," Phys. Rev. Lett. **105**, 174502 (2010).
[21]M. Gad-el Hak, R. Blackwelderf, and J. Riley, "On the growth of turbulent regions in laminar boundary layers," J. Fluid. Mech. **110**, 73 (1981).
[22]B. Singer, "Characteristics of a young turbulent spot," Phys. Fluids **8**, 509 (1996).
[23]J. Wang, J. F. Gibson, and F. Waleffe, "Lower branch coherent states in shear flows: Transition and control," Phys. Rev. Lett. **98**, 204501 (2007).
[24]F. Waleffe, "On a self-sustaining process in shear flows," Phys. Fluids **9**, 883 (1997).

Author complimentary copy. Redistribution subject to AIP license or copyright, see http://phf.aip.org/phf/copyright.jsp